Colloid Polym Sci 279:1144–1148 (2001)

SHORT COMMUNICATION

A. Yoshino
M. Ishida
H. Yuki
H. Okabayashi
H. Masuda
C. J. O'Connor

Structure of liquid-crystalline phases formed by *N*-acetyl-L-glutamic acid oligomeric benzyl esters – ^{2}H NMR study

Received: 27 February 2001
Accepted: 8 May 2001

A. Yoshino · M. Ishida · H. Yuki
H. Okabayashi (✉) · H. Masuda
Department of Applied Chemistry
Nagoya Institute of Technology
Gokiso-cho, Showa-ku, Nagoya
466-8555, Japan

C. J. O'Connor
Department of Chemistry
The University of Auckland, Private Bag
92019, Auckland, New Zealand

Abstract A series of *N*-acetyl-L-glutamic acid oligopeptide benzyl esters with exact residue numbers 4, 6, and 12 has been synthesized by a stepwise procedure. For these oligopeptide–dioxane binary systems, the behavior of the liquid-crystalline phases has been examined by the use of ^{2}H NMR, and the results indicate that highly ordered aggregates formed by these oligopeptides in dioxane are in an alignment similar to that in a nematic mesophase.

Key words *N*-Acetyl-L-glutamic acid oligopeptide benzyl esters · ^{2}H NMR · Liquid-crystalline phase

Introduction

A tremendous number of articles on liquid-crystalline polypeptides have accumulated over the past 45 years, since the time when a liquid-crystalline structure in solutions of poly(γ-benzyl-L-glutamate) (PBLG) was first reported by Elliot and Ambrose [1] and Robinson [2, 3]. Concentrated solutions of rigid α-helical polymers nowadays constitute an increasingly interesting class of lyotropic liquid crystals.

Murthy et al. [4] carried out an intermolecular X-ray scattering analysis [5], in order to obtain the order parameter (S) for magnetically oriented PBLG liquid-crystalline solutions in dioxane and calculated a value of $S \approx 0.75$.

Abe and Yamazaki [6, 7] demonstrated that the technique of ^{2}H NMR is useful for studying the molecular ordering of high-molecular-weight PBLG in the liquid-crystalline state. They elucidated the orientation order parameter of the α-helical backbone as a function of concentration and the most preferred conformation of the side chain by using variously deuterium-labeled PBLG samples.

Most of the articles published on PBLG molecules have focused on high-molecular-weight PBLG, although low-molecular-weight homologs have been described [8, 9]. However, until now the physicochemical properties of low-molecular-weight PBLG remain unresolved.

In this present study, we synthesized, by a stepwise procedure, a series of NH-deuterated *N*-acetyl-L-glutamic acid oligomeric benzyl esters with exact residue numbers of 4, 6, and 12 and examined their liquid-crystalline phase in the oligopeptide–dioxane systems by the use of ^{2}H NMR.

Experimental

Materials

N-Acetyl-L-glutamic acid oligomeric benzyl esters (AN_pZ, $N_p = 4$, 6, and 12) were synthesized by a stepwise procedure [10]. The A4Z and A6Z samples were identified by elemental analysis: agreement between calculated and observed values was within 0.3%. Identification of A12Z was by ^{1}H NMR.

N-deuterated A4Z [A4Z(ND)], A6Z [A6Z(ND)], and A12Z [A12Z(ND)] were prepared as follows. The AN_pZ samples were dissolved in CF_3COOD (trifluoroacetyl-*d*1), and then the solvent was removed in vacuo. This treatment was repeated until the NH stretch band (3,306 cm^{-1}) in the IR spectrum had completely disappeared. The N-deuterated samples thus obtained were recrystallized in CH_2Cl_2–petroleum ether.

X-ray powder diffraction pattern and IR absorption measurements

X-ray powder diffraction patterns were obtained using an RAD-RC diffractometer with a counter–monochromator (CuLα, 50 kV, 110 mA). IR absorption spectra were recorded using a PerkinElmer 1600 FTIR spectrometer (4,000–400 cm^{-1}) with the sample dispersed in KBr discs for the solid states and with the sample–dioxane solutions sandwiched between two CaF_2-plate windows.

^{2}H NMR measurements

^{2}H NMR spectra were measured at 61.4 MHz using a Varian UNITY-400 plus spectrometer at 298 K. A standard two-pulse sequence (S2PUL) was used with an acquisition time of 0.008 s, a pulse width of 12.5 μs and a spectral width of 5.0 MHz. The ^{2}H NMR signals were accumulated 4,096 times for 32,768 data points. The ^{2}H chemical shifts (in parts per million) are given relative to an external deuterated $(CH_3)_3Si(CD_2)_3SO_3Na$.

Results and discussion

The X-ray powder diffraction patterns were measured for the AN_pZ oligomers in the solid state. Lattice spacings were observed in common at 4.71 and 15.85 Å for these solid oligomers and were assigned to the distance between β-sheet-type peptide chains and the side-chain spacing [11], respectively, indicating that these oligomers take up a β-sheet structure in the solid state.

The Fourier transform IR spectra of the AN_pZ oligomers in the solid state were also measured at room temperature and were compared with those of simple amide molecules [12], PBLG [13], and other polypeptides [14, 15]. The amide I and II bands, which were observed in common at 1,684–1,693 and 1,521–1,530 cm^{-1}, respectively, provided evidence that these AN_pZ oligomers take up an antiparallel-type β-sheet structure in the solid state.

For the A4Z–, A6Z–, and A12Z–dioxane systems, we determined the phase maps and examined the phase structures by use of IR, small-angle neutron scattering (SANS), and small-angle X-ray scattering techniques (reported separately). Results of special relevance to this present study may be summarized as follows.

The phase maps of samples of the three systems consist of three common regions (1, 2, and 3). Region 1 is a homogeneous and transparent one-phase solution and is optically isotropic. In region 1 there is a critical aggregation concentration (cac) and above this concentration these oligomeric molecules form rodlike aggregates, in which the antiparallel β-sheet structures, which are stabilized upon aggregation, are stacked one dimensionally. In regions 2 and 3 (bottom layer), highly ordered supramolecular aggregates are formed. Region 2 is the liquid-crystalline phase, and region 3 is a two-phase solution with a transparent upper layer and a turbid (or transparent) and viscous bottom layer. For region 3, it was confirmed that the upper layer is optically isotropic and that the bottom layer is in a liquid-crystalline state. We also identified the colored

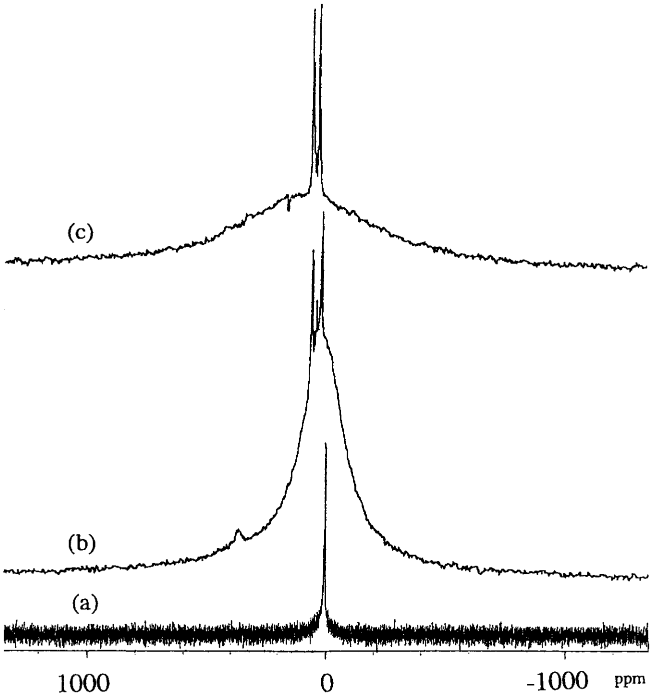

Fig. 1 ^{2}H NMR spectra of the (*a*) A4Z(ND) (40 wt%)–, (*b*) A6Z(ND) (30 wt%)–, and (*c*) A12Z(ND) (28 wt%)–dioxane systems in the liquid-crystalline phase at room temperature (about 298 K)

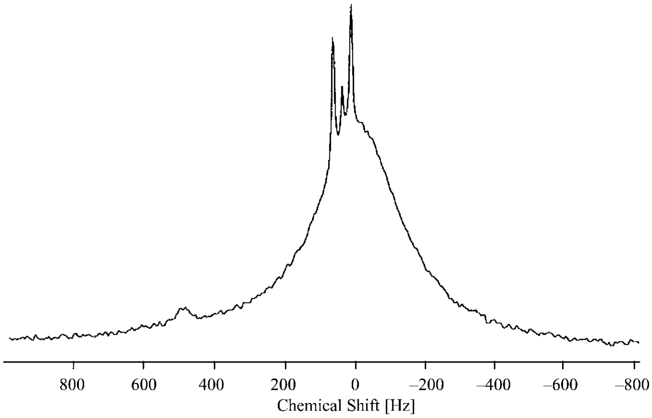

Fig. 2 Expanded ^{2}H NMR spectrum of the A6Z(ND) (30 wt%)–dioxane system in the liquid-crystalline phase (298 K)

regions within regions 2 and 3 (bottom layer) which provide selective light scattering.

In order to understand the aggregate structure in region 2 (particularly, in the colored region), the ^{2}H NMR spectra of the A4Z(ND)–, A6Z(ND)–, and A12Z(ND)–dioxane systems in region 2 were examined. Three sharp signals, superimposed upon a very broad signal, were observed in common, as shown in Figs. 1, spectrum b and 2. The ^{2}H NMR spectrum of the A6Z(ND)–dioxane sample (30.0 wt%) in the liquid-crystalline state, as a representative of the AN_pZ samples, was examined in detail. The expanded ^{2}H NMR spectrum of this sample is shown in Fig. 1, spectrum b. The spectral feature with a resonance line ($\delta \sim 3.27$ ppm; half-height width, $\nu_{1/2}$: 284 Hz) is completely different from the quadrupolar-splitting feature of N-deuterated PBLG in the lyotropic liquid-crystalline state [7]. We may assume that the fractional populations of the three sharp components must be very small, a conclusion consistent with the small integral intensities of these components compared with that of the very broad resonance component. It has been confirmed that the three sharp components do not come from deuterated water molecules, since the ^{2}H resonance line of D_2O in the A6Z–dioxane system, containing a small amount of D_2O, appeared at 3.044 ppm.

We measured the concentration dependence of the ^{2}H NMR spectra for the sample solutions of the AN_pZ–dioxane systems in regions 1 and 2. The concentration dependence of the ^{2}H NMR spectrum for the A6Z–dioxane system is shown in Fig. 3. A very sharp singlet signal (P_m) is observed below the cac (0.5 wt%) and may be assigned to the ^{2}H resonance signal of A6Z(ND) molecules in the monomeric state. Furthermore, as the concentration increases (1, 10, and 15 wt%) above the cac, a relatively broad peak, P_1, appears at high field and its intensity increases with increasing shift towards high field. We may assign P_1 to the small aggregates of A6Z molecules formed at concentrations above the cac. The broadening of the P_1 peak probably results from the fact that formation of the aggregates brings about an increase in the rigidity of the molecules and causes the anisotropy in the chemical shift to increase. The shape of the very broad P_1 signal in the liquid-crystalline phase probably indicates that the molecular axes of aggregation of the A6Z molecule are not aligned in the same direction.

A further increase in concentration brings about a marked variation in the ^{2}H resonance feature. As the intensity of the peak, P_m, decreases with an increase in concentration, two ^{2}H resonance peaks (P_2 and P_2') appear on both sides of the peak P_m, accompanied by an increase in both their intensity and linewidth, until the peak P_m finally disappears and only slightly broadened peaks P_2 and P_2' are found. We emphasize that the broadening of the P_1 peak occurs rapidly with an increase in concentration in the liquid-crystalline region, indicating that formation of the liquid-crystalline structure increases the anisotropic effect of the ^{2}H chemical shift in the aggregates. Further association of the small aggregates may bring about highly ordered aggregates similar in structure to those in a nematic liquid-crystalline phase. It is likely that the monomeric molecules incorporated into the A6Z aggregates are forced to orient under the influence of the liquid-crystalline phase, thereby inducing a small quadrupolar splitting of the ^{2}H resonance line derived from the monomeric molecules. Furthermore, an increase in A6Z concentration and a lowering of temperature bring about an increase in the extent of orientation within the liquid-crystalline phase, leading to an increase in the splitting ($\Delta\nu = \Delta\nu_{P_2} - \Delta\nu_{P_2'}$) of the ^{2}H resonance line.

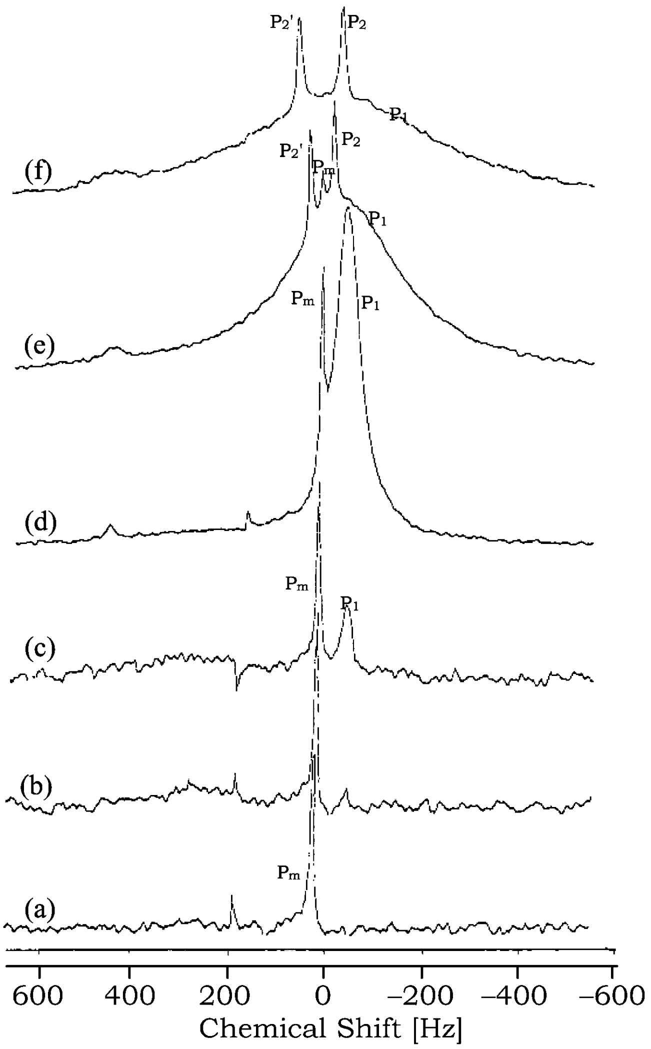

Fig. 3 Concentration dependence of the ^{2}H NMR spectrum of the A6Z(ND)–dioxane system: (*a*) 0.1 wt%, (*b*) 1.0 wt%, (*c*) 10.0 wt%, (*d*) 15.0 wt%, (*e*) 30.0 wt%, and (*f*) 40.0 wt%

In the two-phase region, the ^{2}H NMR spectra were measured in both the upper and bottom layers of the sample solution (28 wt%) (spectra not shown). For the upper layer, only a sharp singlet signal was observed, indicating that the upper layer is an isotropic solution and that the sharp singlet ^{2}H signal may be assigned to A6Z molecules in the monomer state. The bottom layer provides a ^{2}H spectral feature similar to that of the 40 wt% sample (Fig. 2), indicating that the bottom layer is in a liquid-crystalline state.

In order to characterize further the bottom layer, the temperature dependence of the ^{2}H resonance signal was investigated in the liquid-crystalline sample (40 wt%). The half-height width of the very broad ^{2}H signal (P_1) was found to decrease with an increase in temperature, indicating that the mobility of the A6Z molecules in the liquid crystal increases. Furthermore, we note that the relatively sharp ^{2}H resonance signals (P_2, P_2', and P_m), which are superimposed on the broad P_1 signal, are strongly dependent upon temperature. The temperature dependence of the P_2, P_2', and P_m signals is shown in Fig. 4. We found that as the temperature increases a transition from the liquid-crystalline phase to the isotropic phase occurs and that the P_2 and P_2' signals disappear until finally only the P_m signal is observed. We confirmed that the decrease in temperature brings about an inverse variation in intensity. Since the P_m signal comes from the A6Z molecules in the monomeric state, we may assume that the monomeric molecules, which are probably incorporated and oriented between the aggregates, furnish the P_2 and P_2' signals as a consequence of quadrupolar splitting.

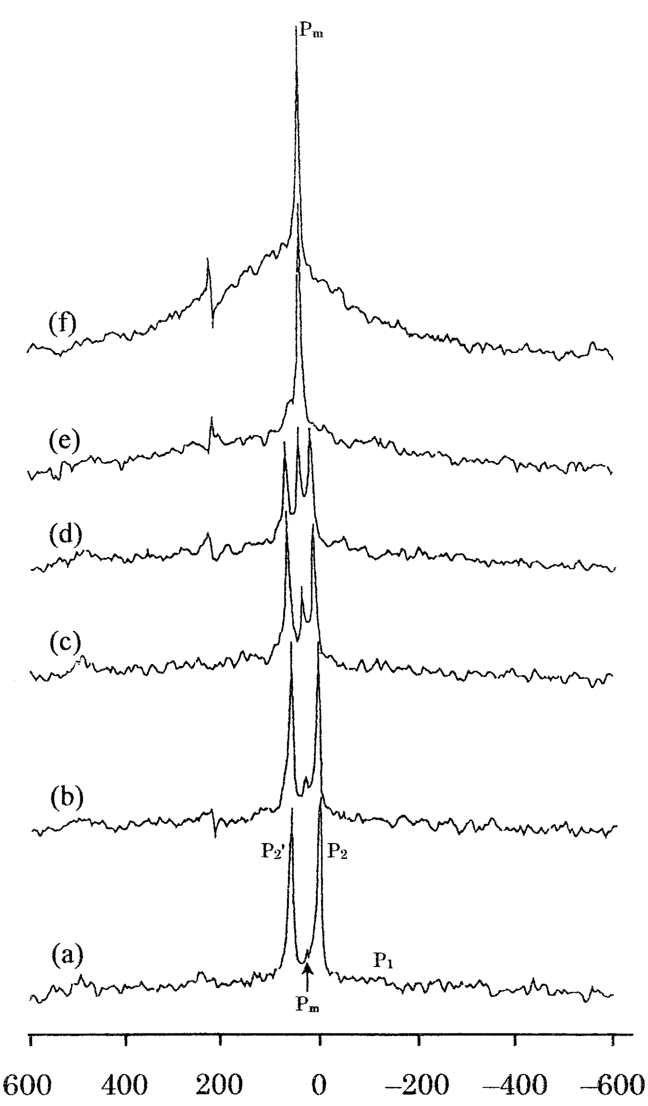

Fig. 4 Temperature dependence of the ^{2}H NMR spectrum of the A6Z(ND) (30.0 wt%)–dioxane system: (*a*) 288 K, (*b*) 293 K, (*c*) 298 K, (*d*) 303 K, (*e*) 308 K, and (*f*) 328 K

It was thought that the ^{2}H NMR behavior of the A6Z molecules in the liquid-crystalline phase might be analogous to the high resolution ^{1}H NMR spectral behavior of the oriented solute molecules dissolved in the nematic liquid crystal [16].

For surfactant molecules, in which the aggregates (i.e., micelles) are formed in aqueous solution above the critical micelle concentration, the ^{2}H NMR spectrum for the isotropic phase of the surfactant–D_2O system provides a narrow singlet ^{2}H signal. When a pseudophase and a single-step model are applied to the isotropic phase, the observed chemical shift (δ) is a weighted average of the chemical shifts in the monomers and the micelles, indicating that the exchange rate of the surfactant molecule between the bulk solution and the micelles is rapid compared with the difference between the δ values of the monomers and micelles [17].

However, this model cannot be applied to the present AN_pZ–dioxane systems, since the ^{2}H NMR spectrum of the sample oligomer–dioxane system consists of distinct signals, as seen in Fig. 2. Therefore, we may assume that the rate of molecular exchange between the oligomers in the monomeric state and the rates in the aggregates is relatively slow [18].

Samulski [19] and Sohma and Tabata [20] measured ^{2}H NMR spectra of PBLG, with partially or fully deuterated benzyl groups, in the lyotropic liquid-crystalline state. They concluded from the observed quadrupolar splitting that the orientation of the side chain is also anisotropic. Abe and Yamazaki [6] observed the quadrupolar splittings ($\Delta\nu$) of the N–D bonds of N-deuterated PBLG ($M_v = 68{,}000$) in the lyotropic liquid-crystalline state ($\Delta\nu_{ND} = 259.0$ kHz (30 °C) in $CHCl_3$, and $\Delta\nu_{ND} = 235.2$ kHz (30 °C) in dimethylformamide, DMF), and determined the order parameters (S) of the α-helical axis [$S = 0.964$ ($CHCl_3$) and $S = 0.875$ (DMF)]. These large quadrupolar splitting values are the result of the orientation of the intramolecular hydrogen-bonded ND groups aligned parallel to the helical axis.

As a consequence of the IR and SANS analysis, we may now present a structural model of the AN_pZ oligomer aggregates, in which antiparallel β-sheet-type

AN_pZ oligomers are stacked one dimensionally through intermolecular hydrogen bonding. Therefore, for the AN_pZ aggregates, the N–D bonds participating in the intermolecular hydrogen bonding may be approximately perpendicular to the molecular axis of a β-sheet oligomer. Such an orientation of the N–D bonds perpendicular to the molecular axis of a β-sheet structure may not be as rigid as the intramolecular hydrogen bonds in the α-helical structure. This difference in rigidity of the hydrogen-bonding system may bring about a fluctuation in the orientation of the N–D bonds, leading to very broad P_1 signals.

Thus, for the A4Z(ND)–, A6Z(ND)–, and A12Z(ND)–dioxane systems, we may conclude that the structure in the liquid-crystalline phase is similar to that in a nematic phase. That is, rodlike aggregates formed by these oligomeric molecules may be aligned in the direction of the long axis of an aggregate but there may be irregularities in alignment in the direction perpendicular to the long axis. A small splitting of ^{2}H signal (P_2 and P_2'), which was observed in the liquid-crystalline phase of the AN_pZ–dioxane system, may arise from the restricted state of the monomeric molecules incorporated into the AN_pZ aggregates.

References

1. Elliot A, Ambrose EJ (1950) Discuss Faraday Soc 9:246
2. (a) Robinson C (1956) Trans Faraday Soc 52:571; (b) Robinson C (1961) Tetrahedron 13:219; (c) Robinson C (1966) Mol Cryst 1:467
3. Robinson C, Ward JC, Beevers RB (1958) Disc Faraday Soc 25:29
4. Murthy NS, Knox JR, Samulski ET (1976) J Chem Phys 65:4835
5. Alexander LE (1969) X-ray diffraction methods in polymer science. Wiley-Interscience, New York, p 241
6. Yamazaki T, Abe A (1987) Polym J 19:777
7. (a) Abe A, Yamazaki T (1989) Macromolecules 22:2138; (b) Abe A, Yamazaki T (1989) Macromolecules 22:2145
8. (a) Doty P, Bradbury JH, Holtzer AM, Blout ER (1954) J Am Chem Soc 76:4493; (b) Doty P, Bradbury JH, Holtzer AM (1956) J Am Chem Soc 78:947
9. (a) Masuda Y, Miyazawa T (1967) Makromol Chem 103:261; (b) Blout ER, Asadourian A (1956) J Am Chem Soc 78:955
10. Uehara T, Okabayashi H, Taga K, Yoshida T, Kojima H (1991) J Chem Soc Faraday Trans 88:3451
11. Imae T, Ikeda S (1981) Mol Cryst Liq Cryst 65:73
12. (a) Miyazawa T, Shimanouchi T, Mizushima S (1956) J Chem Phys 24:408; (b) Miyazawa T, Shimanouchi T, Mizushima S (1958) J Chem Phys 29:611
13. (a) Ambrose EJ, Elliott A (1950) Proc R Soc Lond Ser A 205:47; (b) Elliott A (1954) Proc R S Lond Ser A 221:104
14. Miyazawa T, Blout ER (1961) J Am Chem Soc 83:712
15. (a) Fergason JL (1966) Mol Cryst 1:293; (b) Fergason JL, Goldberg NN, Nadalin RJ (1966) Mol Cryst 1:309
16. (a) Saupe A, Englert G (1963) Phys Rev 11:462; (b) Englert G, Saupe A (1964) Z Naturforsch A 19:172; (c) Saito K, Yoshino A, Yoshida T, Takahashi K (1983) Bull Chem Soc Jpn 56:3585; (d) Saito K, Yoshino A, Yoshida T, Takahashi K (1992) Bull Chem Soc Jpn 65:1135; (e) Saito K, Hattori E, Nozaki M, Yoshino A, Takahashi K (1994) Bull Chem Soc Jpn 67:912
17. Khan A, Fontell K, Lindblon G, Lindman B (1982) J Phys Chem 86:4266
18. Gutowsky HS, Holm CH (1956) J Chem Phys 25:1228
19. Samulski ET (1979) J Phys (Paris) 40:C3–471
20. Sohma J, Tabata M (1981) Mol Cryst Liq Cryst 68:89